Electronic Supplementary Information:

Inflammatory response induced by synergistic interactions between nanoplastics and typical heavy metal ions in human cells

Cong Li[1], Xinxin Huang[1], Weicui Min[1, 2], Huoqing Zhong[1], Xiliang Yan[1], Yan Gao[1, 2], Jianqiao Wang[3], Hongyu Zhou[1]*, Bing Yan[1]*

[1] Institute of Environmental Research at Greater Bay, Key Laboratory for Water Quality and Conservation of the Pearl River Delta, Ministry of Education, Guangzhou University, Guangzhou, Guangdong, 510006, China

[2]School of Environmental Science and Engineering, Shandong University, Qingdao, Shandong, 250100, China

[3]School of Environmental Science and Engineering, Guangzhou University, Guangzhou, 510006, China

***Corresponding author**

Bing Yan (drbingyan@yahoo.com); Hongyu Zhou (hyzhou001@gzhu.edu.cn)

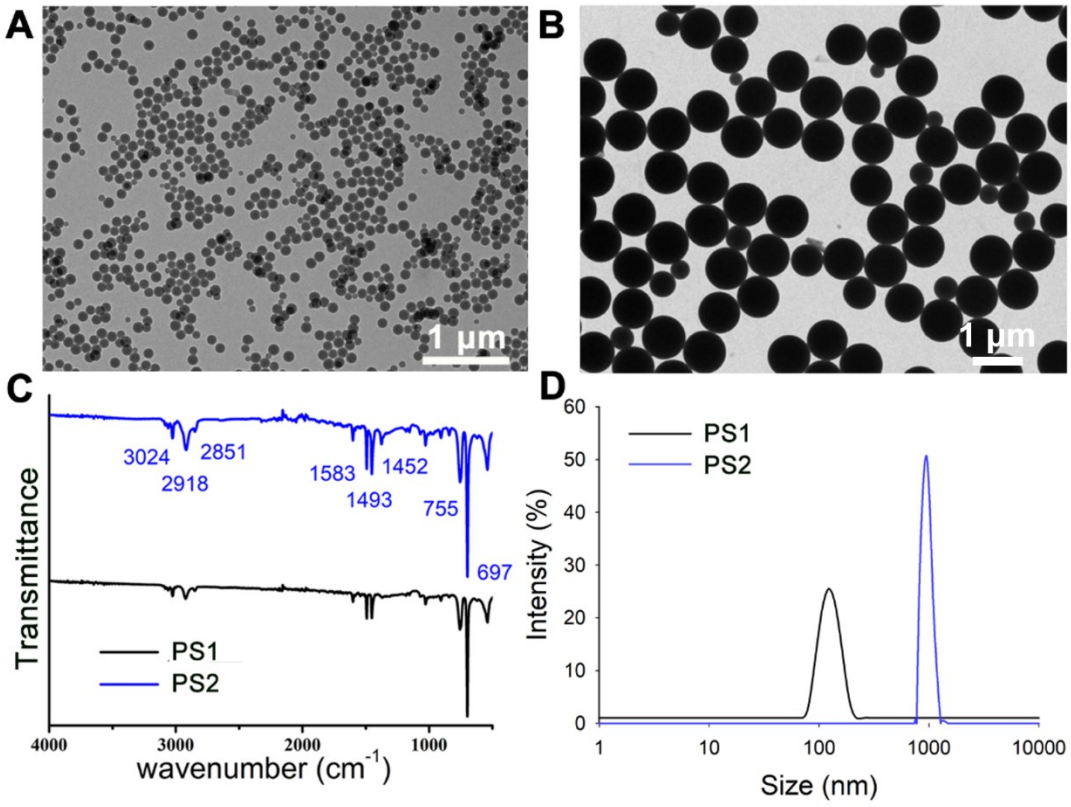

Fig. S1. Characterization of PS1 and PS2. (A-B) TEM images of PS1 and PS2; (C) FTIR spectra of PS1 and PS2; (D) Hydrodynamic diameters of PS1 and PS2 in deionized H_2O.

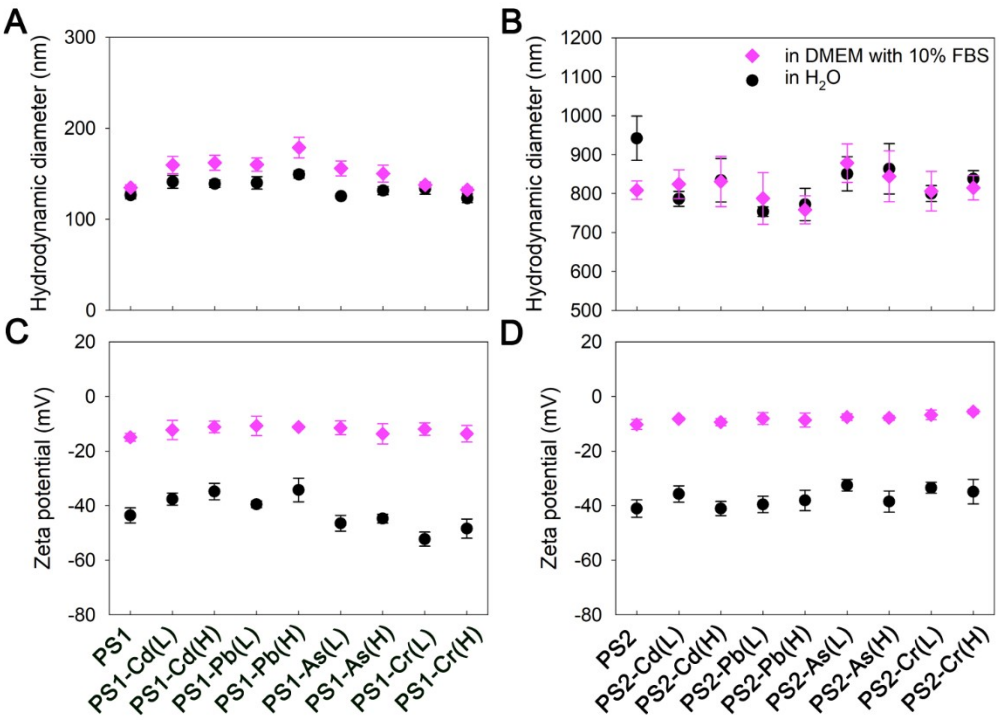

Fig. S2. Characterization of PS1-ions and PS2-ions. Hydrodynamic diameters of (A) PS1-ions and (B) PS2-ions in deionized H_2O and DMEM with 10% FBS. Zeta potentials of (C) PS1-ions and (D) PS2-ions in deionized H_2O and DMEM with 10% FBS. The concentration of PS is 100 μg/mL. (mean ± SD, n = 3).

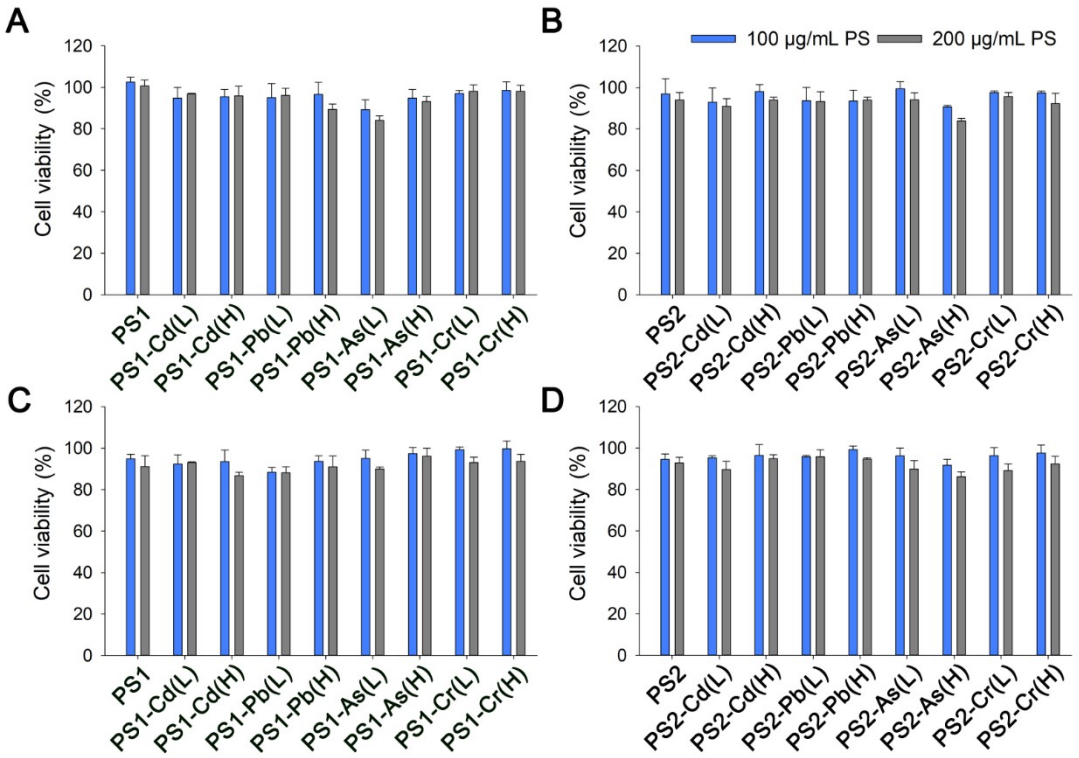

Fig. S3. Cell viability (A, B) Caco-2 cells and (C, D) THP-1 macrophages upon exposure to PS NPs or PS-ions. Cells were treated with 100 and 200 μg/mL PS1, PS2, PS1-ions, or PS2-ions for 48 h. No obvious cytotoxicity was observed after exposure to PS-ions in both cell lines (mean ± SD, n = 3).

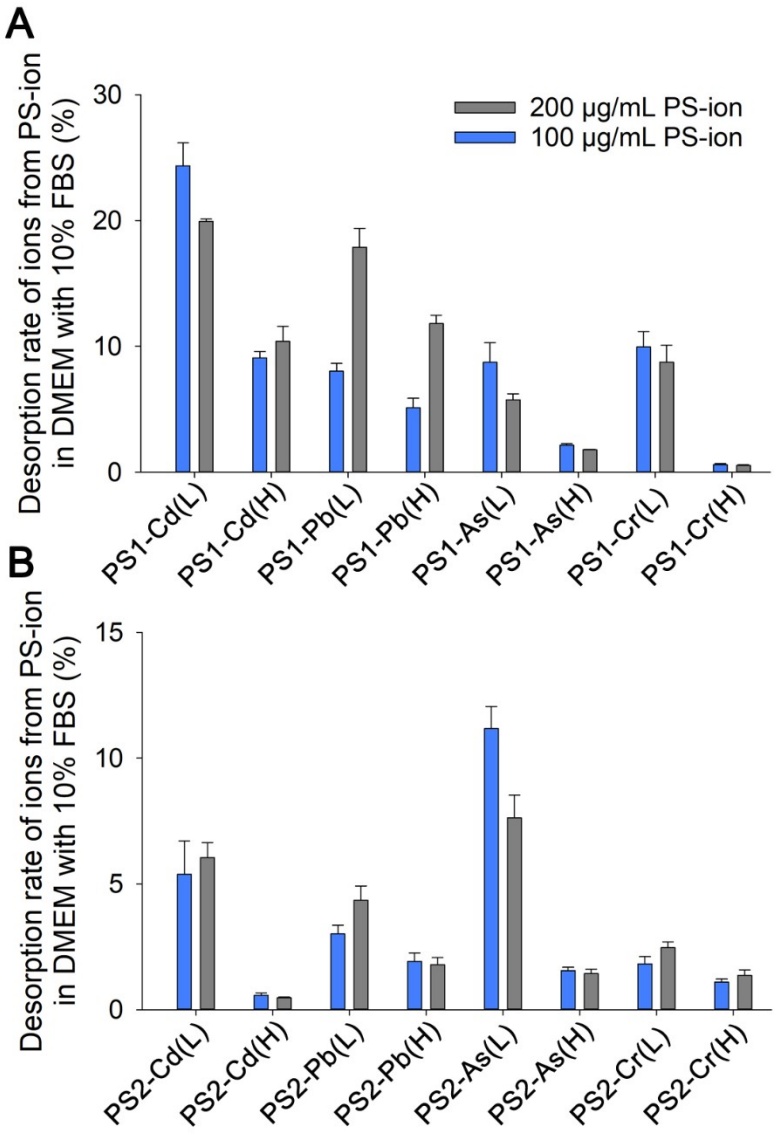

Fig. S4. Desorption rates of each ions from 100, 200 μg/mL (A) PS1-ions and (B) PS2-ions in DMEM with 10% FBS for 48 h (mean ± SD, n = 3). The desorption concentrations of Cd^{2+}, Pb^{2+}, As(III), and Cr(VI) in 200 μg/mL PS1-ions(H) were 45, 150, 10, and 15 ng/mL, respectively.

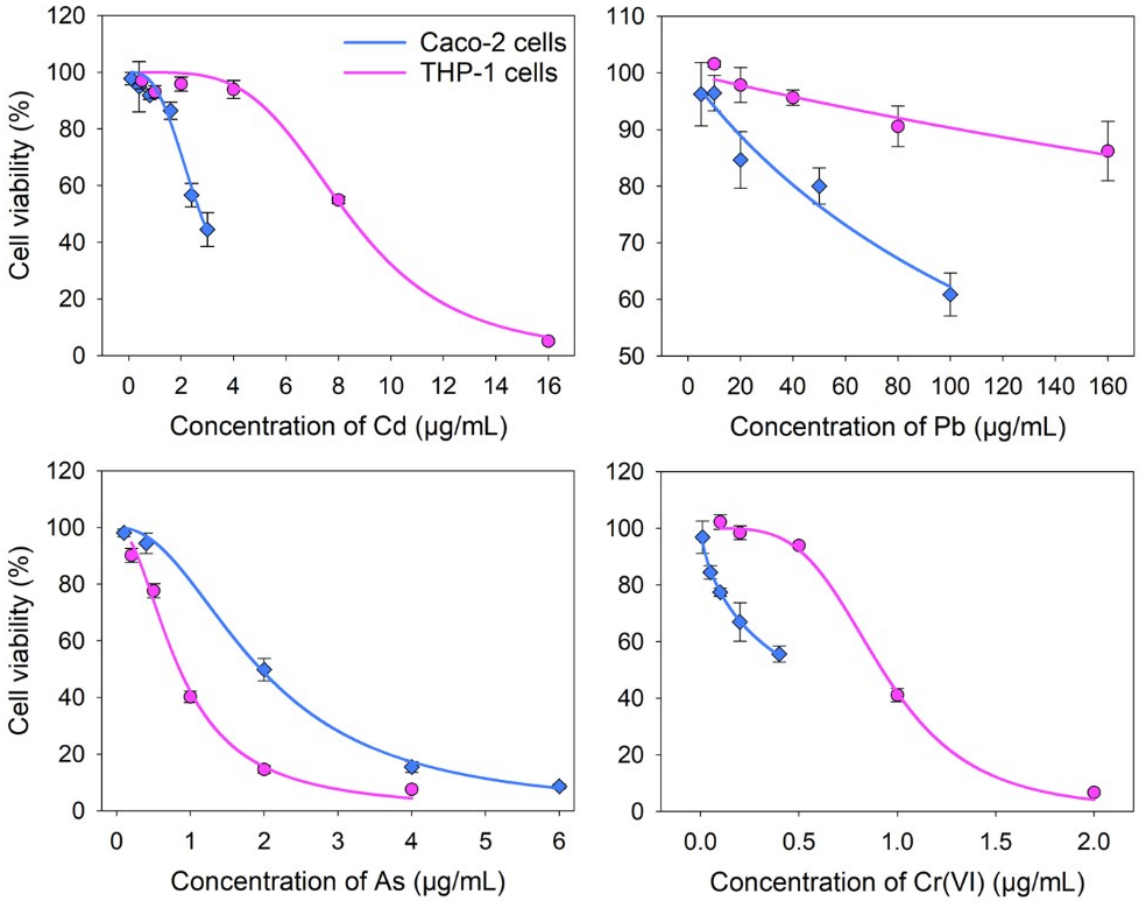

Fig. S5. Cell viability of Caco-2 and THP-1 macrophages exposed to Cd^{2+}, Pb^{2+}, As(III), and Cr(VI) with various concentrations for 48 h.

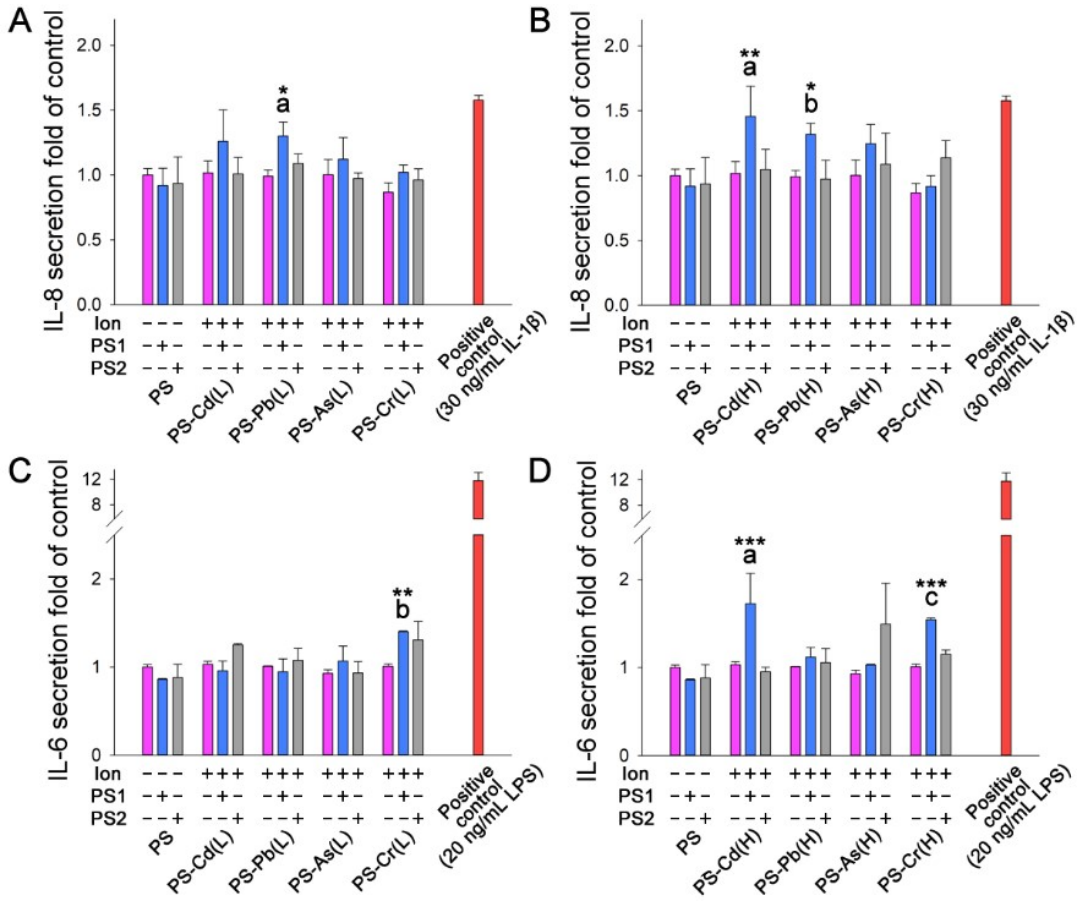

Fig. S6. Combined effects of PS-ions on the secretion of inflammatory cytokines. IL-8 secretion in Caco-2 cells exposed to 100 μg/mL (A) PS-ion(L) and (B) PS-ion(H) for 48 h. IL-6 secretion in THP-1 macrophages induced by 100 μg/mL (C) PS-ion (L) and (D) PS-ion (H) for 48 h. The concentrations of individual ions for Pb^{2+}, Cd^{2+}, As(III), and Cr(VI) were 45, 150, 10, and 15 ng/mL. *, **, and *** indicate statistically significant differences compared to PS controls and a, b, and c represent statistically significant differences from corresponding ions (*/a, **/b, and ***/c show $P < 0.05$, $P < 0.01$, and $P < 0.001$, respectively. Mean ± SD, n = 3).

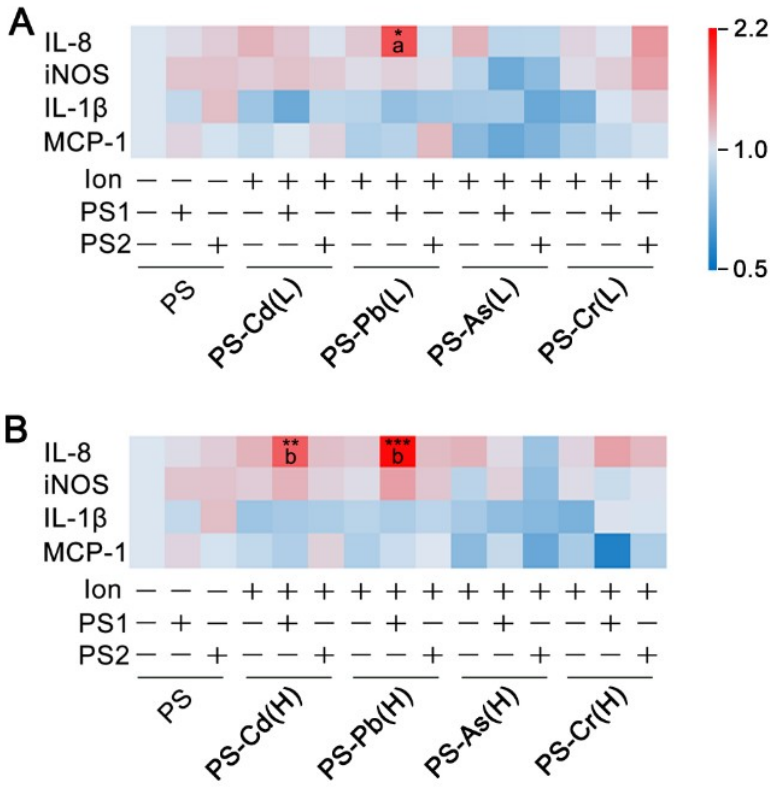

Fig. S7. Gene expression of inflammatory cytokines in Caco-2 cells exposed to 100 μg/mL PS-ions for 48 h. Heat map of mRNA levels for IL-8, iNOS, IL-1β, MCP-1 after the exposure to (A) PS-ion(L) and (B) PS-ion(H). The gene expression is determined by qPCR and fold changes were normalized to negative control. *, **, and *** indicate statistically significant differences compared to PS controls and a, b, and c represent statistically significant differences from corresponding ions (*/a, **/b, and ***/c show $P < 0.05$, $P < 0.01$, and $P < 0.001$, respectively. Mean ± SD, n = 4).

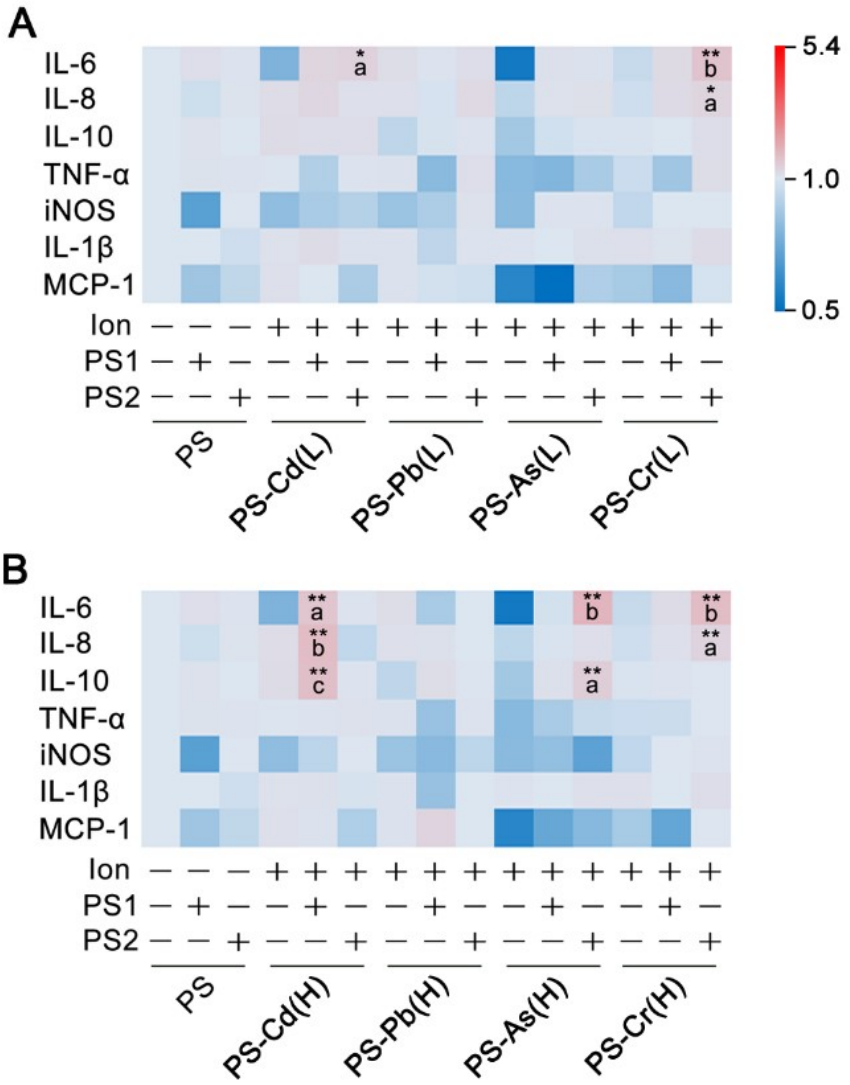

Fig. S8. Gene expression of inflammatory cytokines in THP-1 macrophages exposed to 100 μg/mL PS-ion for 48 h. Heat map of mRNA levels for IL-6, IL-8, IL-10, TNF-α, iNOS, IL-1β, MCP-1 after the exposure to (A) PS-ion(L) and (B) PS-ion(H). The gene expression is determined by qPCR and fold changes were normalized to negative control. *, **, and *** indicate statistically significant differences compared to PS controls and a, b, and c represent statistically significant differences from corresponding ions (*/a, **/b, and ***/c show $P < 0.05$, $P < 0.01$, and $P < 0.001$, respectively. Mean ± SD, n = 4).

Table S1 Sequences of genes analyzed by qPCR

Gene	Forward 5′-3′ primer	Reverse 5′-3′ primer
IL-8	ATGACTTCCAAGCTGGCCGTGGCT	TCTCAGCCCTCTTCAAAAACTTCTC
iNOS	AGGGATTTTAACTTGCAGGTCC	AGGAGCCGTAATATTGGTTGACA
IL-1β	AGCTGGAGAGTGTAGATCCCAA	TGTTTTCTGCTTGAGAGGTGCT
MCP-1	CAGCCAGATGCAATCAATGCC	TGGAATCCTGAACCCACTTCT
IL-6	GAAAGCAGCAAAGAGGCACT	TTTCACCAGGCAAGTCTCCT
IL-10	GTGATGCCCCAAGCTGAGA	CACGGCCTTGCTCTTGTTTT
TNF-α	TCTTCTCGAACCCCGAGTGAC	GGTACAGGCCCTCTGATGGC
β-actin	TTTTAGGATGGCAAGGGACTT	GATGAGATTGGCATGGCTTTA
GAPDH	ATCACCATCTTCCAGGAGCGA	CCTTCTCCATGGTGGTGAAGAC

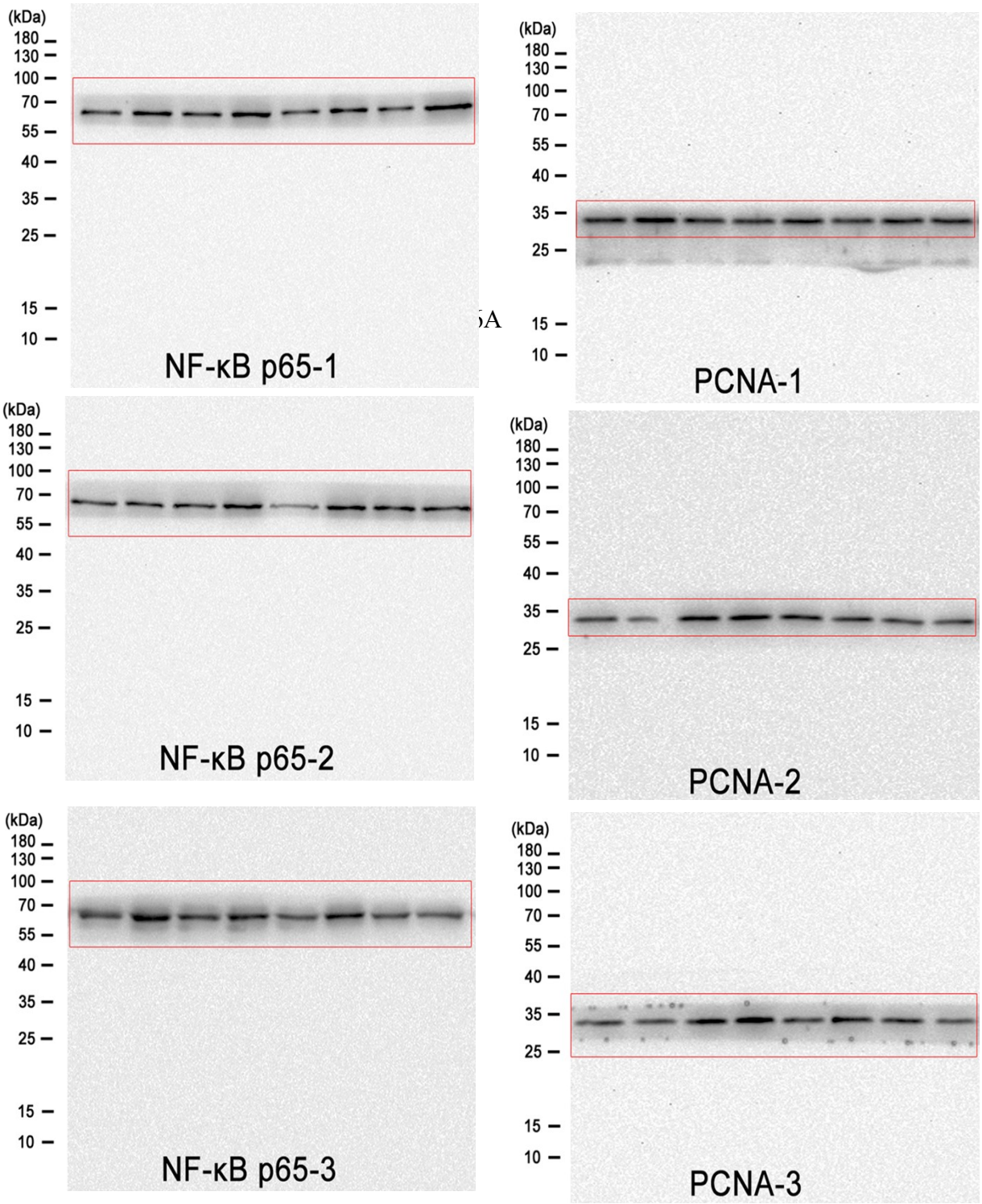

Fig S9 Full Western Blot data for Figure 6A

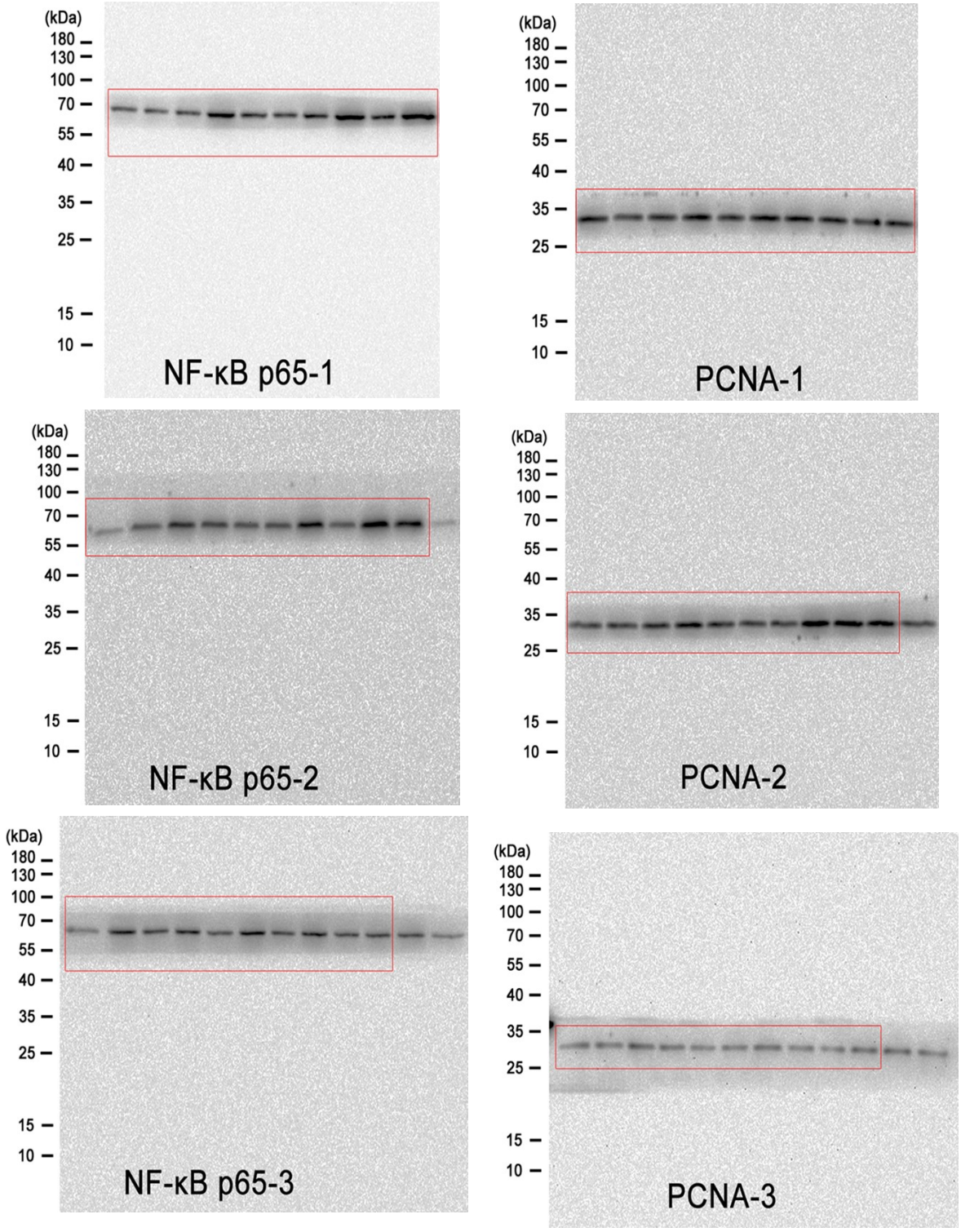

Fig S10 Full Western Blot data for Figure 6B

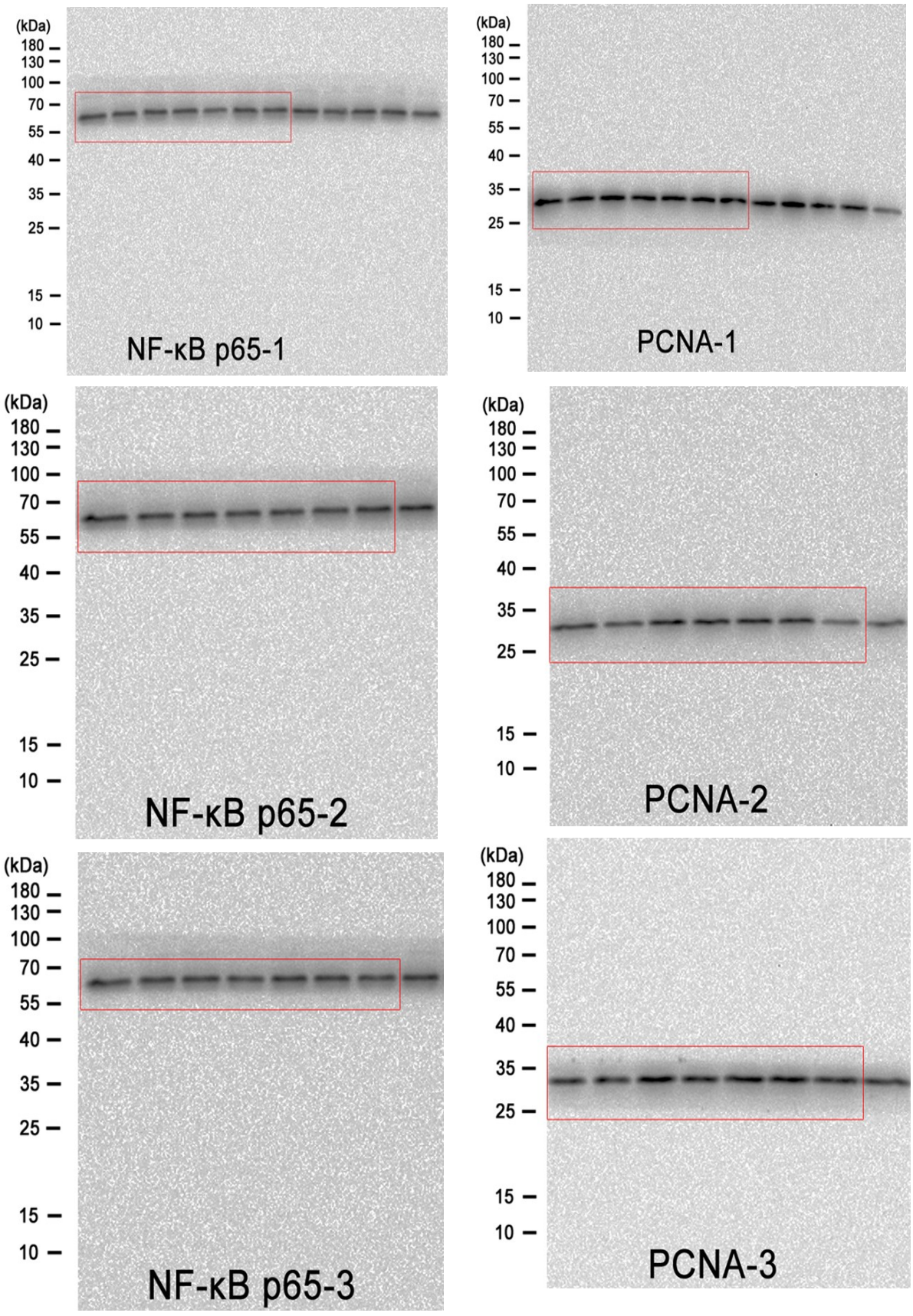

Fig S11 Full Western Blot data for Figure 7A

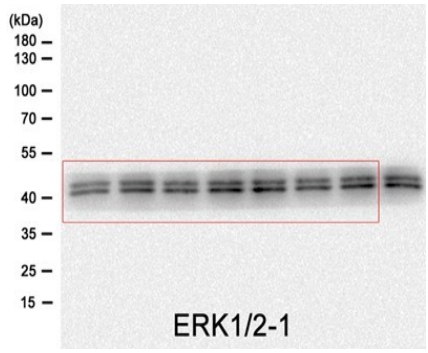
(kDa)
180
130
100
70
55
40
35
25
15
ERK1/2-1

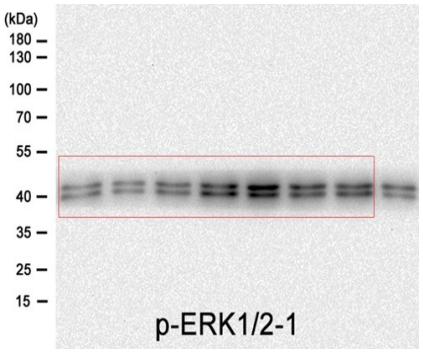
(kDa)
180
130
100
70
55
40
35
25
15
p-ERK1/2-1

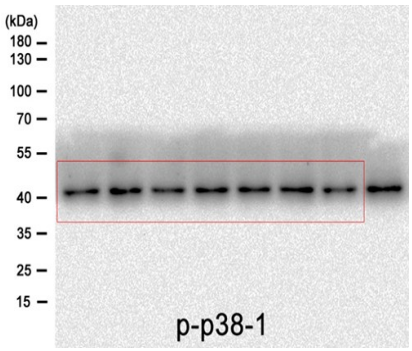
(kDa)
180
130
100
70
55
40
35
25
15
p-p38-1

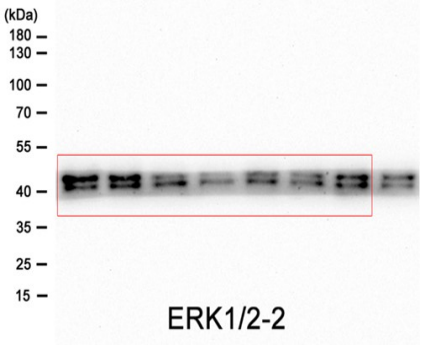
(kDa)
180
130
100
70
55
40
35
25
15
ERK1/2-2

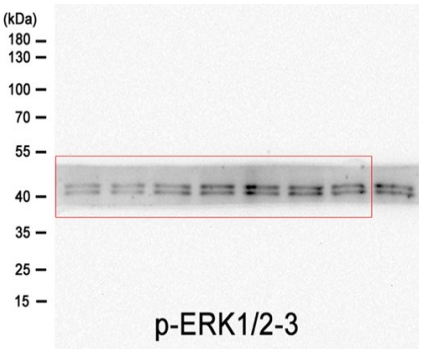
(kDa)
180
130
100
70
55
40
35
25
15
p-ERK1/2-3

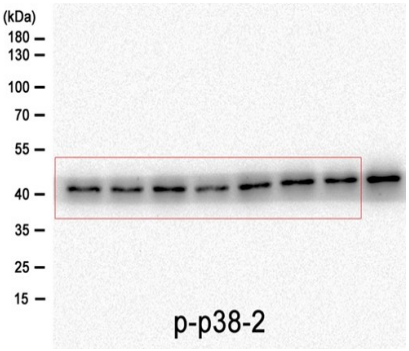
(kDa)
180
130
100
70
55
40
35
25
15
p-p38-2

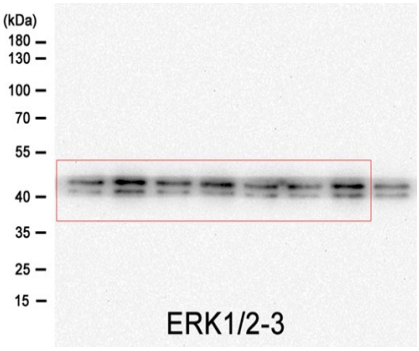
(kDa)
180
130
100
70
55
40
35
25
15
ERK1/2-3

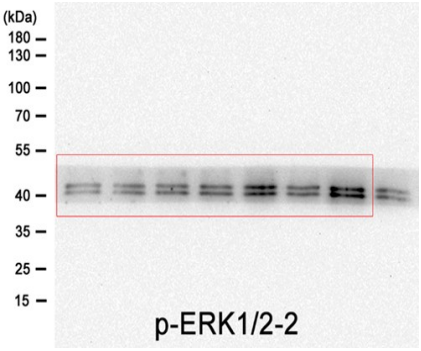
(kDa)
180
130
100
70
55
40
35
25
15
p-ERK1/2-2

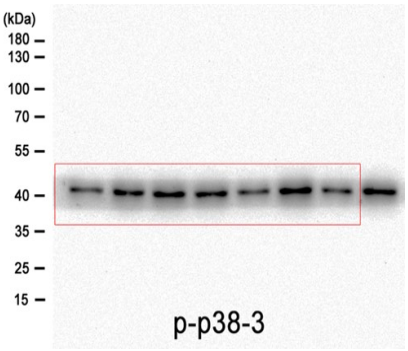
(kDa)
180
130
100
70
55
40
35
25
15
p-p38-3

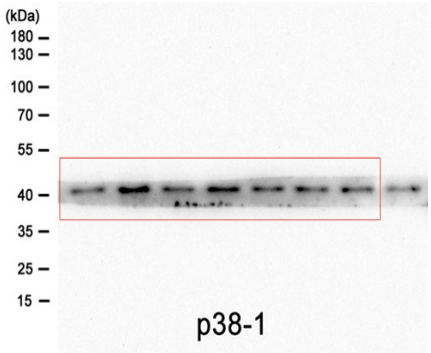
(kDa)
180
130
100
70
55
40
35
25
15
p38-1

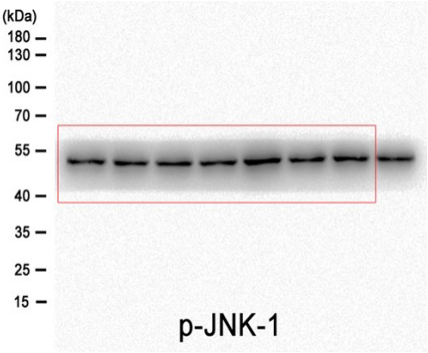
(kDa)
180
130
100
70
55
40
35
25
15
p-JNK-1

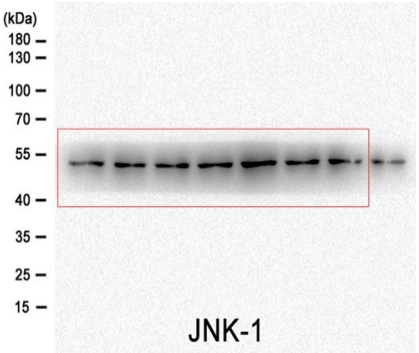
(kDa)
180
130
100
70
55
40
35
25
15
JNK-1

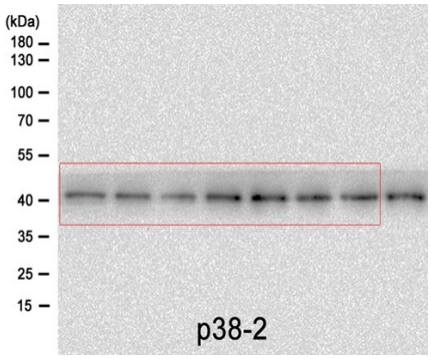
(kDa)
180
130
100
70
55
40
35
25
15
p38-2

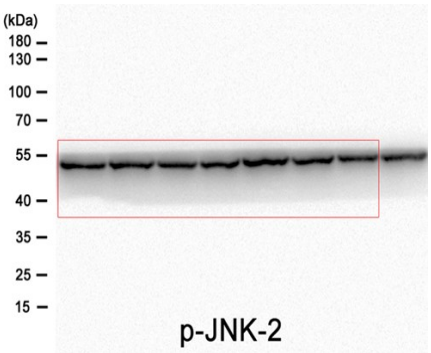
(kDa)
180
130
100
70
55
40
35
25
15
p-JNK-2

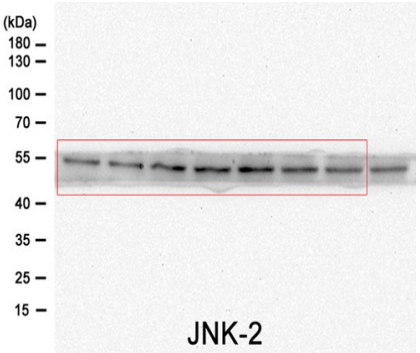
(kDa)
180
130
100
70
55
40
35
25
15
JNK-2

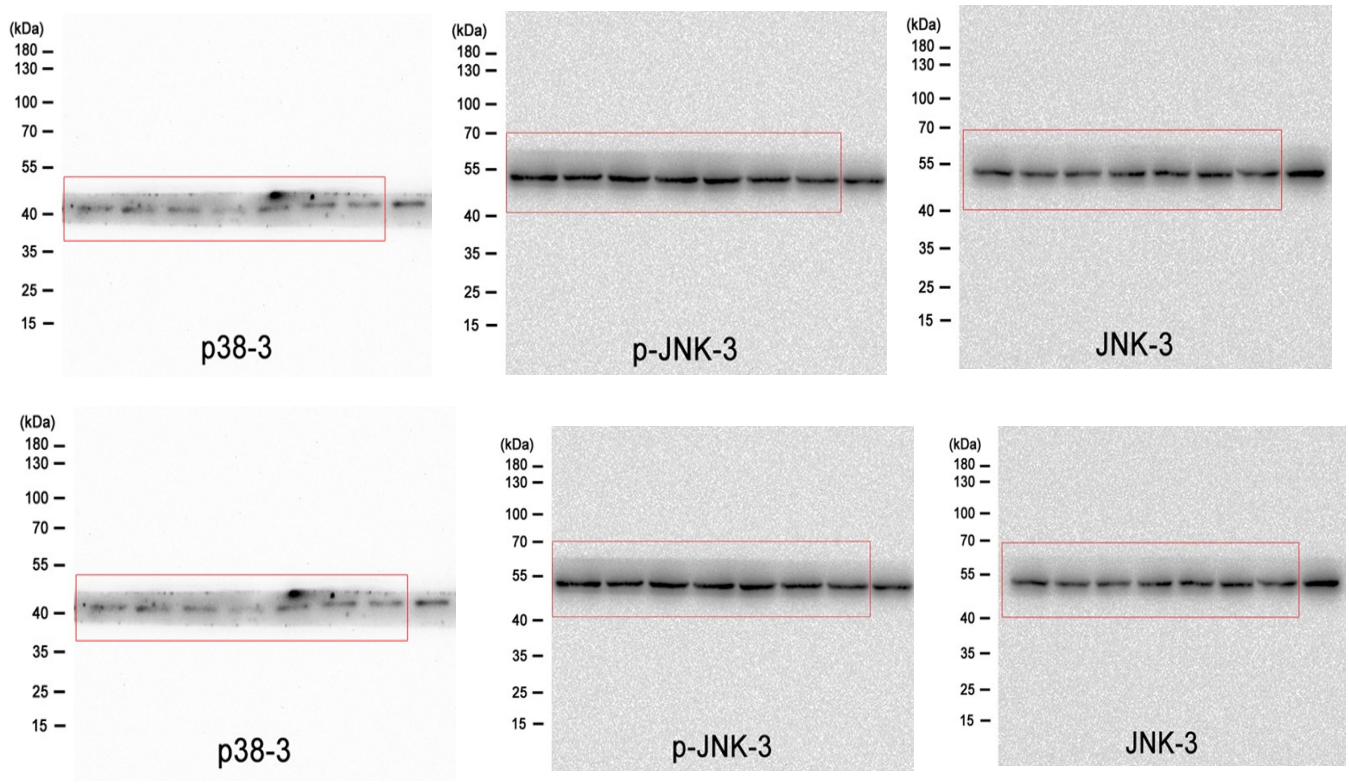

Fig S12 Full Western Blot data for Figure 7B